

Chemical dynamics in interstellar ice

Patrice Theulé 

Laboratoire d'Astrophysique de Marseille
Aix-Marseille University, CNRS, CNES, Marseille, France
email: patrice.theule@univ-amu.fr

Abstract. Chemistry in the interstellar medium is generally out-of-equilibrium and as such is kinetically controlled by a set of time-dependent equations, both for gas-phase chemistry and solid-state chemistry. The competition between the different possible reactions will determine toward which complex molecules the chemical network is driven to. The formation of complex molecules on the surface of the grains or in the ice mantle covering them is set by the diffusion-reaction equation, which is depending on temperature dependent reaction rate constants and diffusion coefficients. This paper shows how these two parameters can be experimentally determined by laboratory experiments. It also shows how the ice mantle reorganization plays an important role in the trapping and reactivity, which leads to the formation of complex organic molecules.

Keywords. astrochemistry, molecular processes, methods: laboratory

1. Introduction

Observations keep reporting an ever increasing molecular complexity, and diversity, in the interstellar medium (ISM), in the circumstellar medium, and in comets (Caselli & Ceccarelli 2012). Interstellar complex organic molecules (iCOMs) are observed by radio astronomy both in hot cores and hot corinos (Bacmann *et al.* 2012), associated with high- and low-mass star formation, respectively. Recent space missions to solar system bodies also reported the abundances of several iCOMs, for example the Cassini-Huygens mission (Gudipati *et al.* 2015). Recently, the COSAC instrument on the ROSETTA mission to comet 67P/Churyumov-Gerasimenko reported several organic compounds, including numerous carbon and nitrogen-rich molecules, in cometary ices (Goesmann *et al.* 2015). Meteorite samples also exhibit an incredibly rich molecular composition in which amino acids have been detected (Ehrenfreund & Charnley, 2000). A large network of chemical reactions exist, both in the gas-phase and in the solid-state, to explain this molecular complexity. Chemistry in the ISM is out-of-equilibrium and is driven by the kinetic rates of the competing reactions at play. As a consequence, the dynamics of the reactions is as important as the network of the reactions to determine the abundances of the formed iCOMs. The dynamics of solid-state chemistry is important to increase the molecular complexity since grains offer a place where molecules can meet and react, act as a third body that can evacuate the excess energy released by exothermic reactions, and sometimes plays a catalytic role by potentially lowering the activation energies of reactions (Potapov *et al.* 2019).

Grain chemistry is described by a Langmuir-Hinshelwood process and its dynamics is modelled by the 2D or 3D reaction-diffusion equation, for reactions on the surface of the grains or for reactions inside the ice mantle of the grains, respectively.

$$\frac{\partial n(\vec{r}, t)}{\partial t} - D(T) \times \delta n(\vec{r}, t) + k(T) f(n(\vec{r}, t)) = 0, \quad (1.1)$$

where $n(\vec{r}, t)$ is the concentration vector of the reactants, $D(T)$ and $k(T)$ the temperature dependent diffusion coefficient and reaction rate constant matrices, respectively and $f(n(\vec{r}, t))$ a function of the concentration of the reactants. We need to know both the diffusion coefficient $D(T)$ of each reactant and the reaction rate constant $k(T)$ for each reaction in order to solve this equation and determine the abundance of all the species as a function of time.

In order to understand Eq. 1.1, we can consider the two extreme cases: (i.) the activation-controlled regime where the reaction timescale is much larger than the diffusion timescale of the reactants, since the larger timescale limits the kinetics of the reaction and (ii.) the diffusion-controlled regime where the diffusion timescale of the reactants is much larger than their reaction timescale. We will see how it is possible to measure $k(T)$ and $D(T)$ independently by performing laboratory experiments in these two regimes.

2. The activation-controlled regime

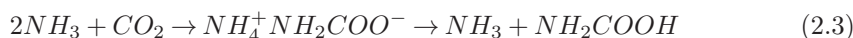
This extreme case is best exemplified by reactions with no diffusion. In the solid-state molecule-molecule (Theulé *et al.* 2013) and molecule-radical (Oba *et al.* 2012; Borget *et al.* 2017) reactions the reactants are located on neighboring sites. As a consequence they do not necessarily need to undergo a translational diffusion since they are already one next to another. The kinetics of such a bimolecular reaction ($A + B \rightarrow C + D$) is given by simplifying Eq. 1.1:

$$\frac{dn(A, t)}{dt} = -k(T)n(A, t)^\alpha n(B, t)^\beta \quad (2.1)$$

where α and β are the partial orders of the reaction. The temperature dependence of the reaction rate constant is given by an Arrhenius law:

$$k(T) = k_0 \times \exp\left(-\frac{E_A}{RT}\right) \quad (2.2)$$

where k_0 is the pre-exponential factor, R (in s^{-1}) the ideal gas constant and E_A the activation energy of the reaction (in kJ mol^{-1} here). A model reaction for such diffusionless activation-controlled reactions is the nucleophilic addition of ammonia and carbon dioxide, which gives ammonium carbamate, which sequentially gives ammonia and carbamic acid



Laboratory studies (Bossa *et al.* 2009, Noble *et al.* 2014, Potapov *et al.* 2019) of the reaction enable to experimentally measure the partial orders α and β , the pre-exponential factor k_0 and the E_a activation energy of the reaction. Note *i.* that the pre-exponential factor k_0 is not equal to 10^{12}s^{-1} if the reaction is not an elementary process, several elementary steps being hidden in k_0 (Noble *et al.* 2014), and *ii.* the rate constant value can depend on the surface (Potapov *et al.* 2019). Kinetic parameters have been measured in laboratory for several reactions (Theulé *et al.* 2013).

3. The diffusion-controlled regime

The other extreme case, the diffusion-controlled regime, the reactivity is driven by the diffusion of the reactants. It is typically the case for radical-radical reactions, which have zero activation energies, where the reactants are far apart and need to diffuse to get one next to another. Thus, the diffusion of the radical reactants is the limiting factor,

as their reactivity is extremely fast in comparison and the reactivity term disappears from Eq. 1.1, which transforms into an usual Fick's second law:

$$\frac{\partial n(\vec{r}, t)}{\partial t} = D(T) \times \delta n(\vec{r}, t) \quad (3.1)$$

Determining, experimentally or theoretically, the diffusion coefficients, both on a surface (2D diffusion) or in a volume (3D diffusion) is quite challenging (Theulé *et al.* 2018). From earlier experiments using laser resonance desorption (Livingston *et al.* 2002) several isothermal experiments of bulk diffusion-desorption (Mispelaer *et al.* 2013; Karssemeijer *et al.* 2014), bulk diffusion-spectroscopic change (Cooke *et al.* 2018; He *et al.* 2018) or diffusion-reactivity (Ghesquière *et al.* 2018) have been performed. These works are indirect, as they use desorption, the change in an absorption band or reactivity (the detection of the formed product) to trace diffusion in a multilayer ice, rather than directly imaging the diffusion of particles, which is the standard method in material sciences. They therefore need molecular dynamics calculations (Karssemeijer *et al.* 2014; Ghesquière *et al.* 2015) to give a microscopic insight. Measuring the temperature dependence of the diffusion coefficient enables the derivation, from an Arrhenius law $D(T) = D_0 \times \exp(-\frac{E_d}{RT})$, of the diffusion pre-exponential factor D_0 (in cm^2s^{-1}) and of the activation energy for diffusion, E_d (in kJ mol^{-1} here), which can be compared to the activation energy for desorption for the corresponding molecules.

However, all these works measure percolation, which is the bulk diffusion in a porous material. Genuine bulk diffusion (either Schottky or Frenkel mechanisms) is much slower than what is measured. The percolation diffusion rates derived from these experiments can be expressed as bulk diffusion coefficients per unit of thickness but they depend on the morphology (porosity, compacity, amorphous to crystalline or polycrystalline ratio) as molecules diffuse along pore walls of undefined length distribution. They can also be expressed as surface diffusion coefficients but also on an undefined surface length scale. Even if this entanglement of bulk diffusion and surface diffusion is hard to resolve, these works give an estimate of the diffusion coefficients.

An important point is that at the constant temperature diffusion-desorption, diffusion-spectroscopic change and diffusion-reactivity experiments are performed the ice mantle morphology is susceptible to change on the timescale of the measurement. At low temperature (below 50 K) the amorphous porous ice can compact, pores can collapse, while at higher temperature (above 120 K) amorphous ice can become crystalline. This morphology changes affect the effective surface area at play during percolation. Reliable measurements can be performed for volatile molecules (CO , CH_4 , O_2) at temperature low enough that the diffusion timescale is much faster than morphological changes.

4. The influence of the water ice mantle structural evolution in the reaction-diffusion

The morphological changes of the water ice mantle is known to trap volatile reactants (Collings *et al.* 2004; Viti *et al.* 2004), which can be brought to a temperature high enough that small activation barriers of reactivity can be overcome (Theulé *et al.* 2013). In addition to the collapse of the pores at low temperature (below 50 K), which is responsible of the trapping of volatiles, the opening of cracks during the crystallization process dramatically increase the effective surface available for percolation. The kinetics studies of the ammonium carbamate formation (Eq. 2.3), where a Langmuir-Hinshelwood mechanism is imposed by the large dilution of the two reactants in a water ice (Ghesquière *et al.* 2018), show that the reaction-diffusion kinetics, as displayed in Fig. 1, is intimately bound to the water ice mantle structural evolution, which is a mixed of pore collapse,

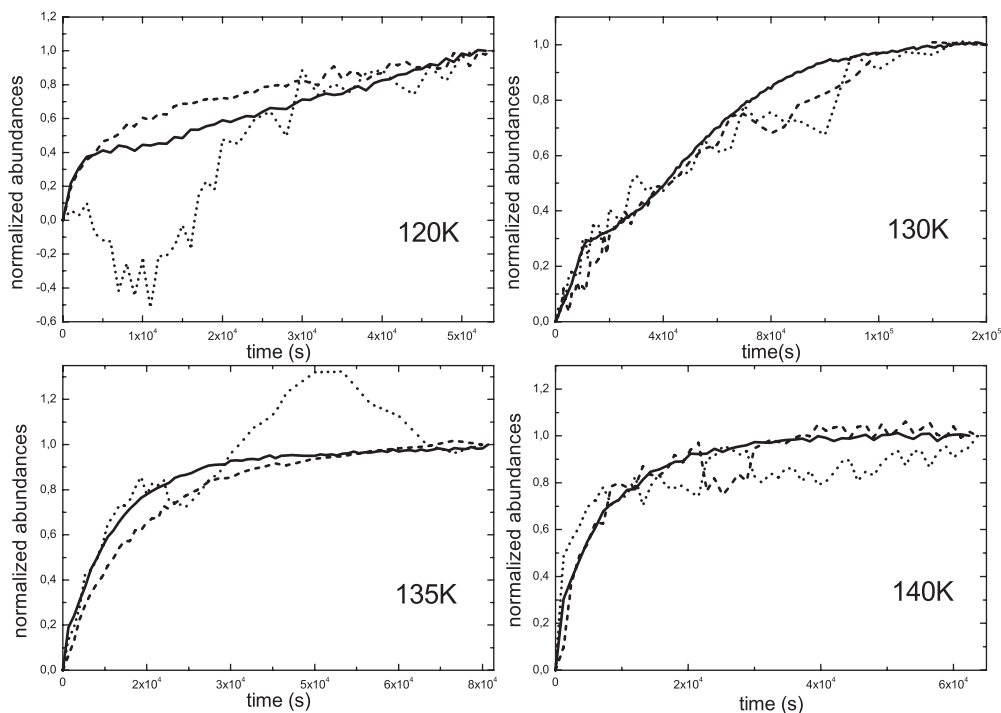


Figure 1. Kinetics of the decay of the CO_2 reactant (dashed line, the decay is flipped for a better comparison), of the formation of the ammonium carbamate product (dotted line), and of the structural evolution of amorphous water ice (solid line) at different temperatures from 120 K to 140 K. At each temperature, the kinetics are obtained by recording the time evolution of the characteristic IR bands of both the reactants and product. Taken from [Ghesquière *et al.* \(2018\)](#).

cracks opening and crystallization. The increased amount of surface available for reactants diffusion during the crystallization process dramatically enhances reactivity, similarly to the so-called "molecular volcano desorption" effect ([Smith *et al.* 1997](#)). The reaction-diffusion kinetics of thermal reactions in bulk water ice is therefore totally dominated by the water ice mantle restructuration kinetics.

5. Conclusion

The dynamics of the out-of-equilibrium low-temperature chemistry on grains is ruled by the reaction-diffusion equation describing a Langmuir-Hinshelwood mechanism, both on a surface and in the mantle of the ice. The comparison between the diffusion and reactivity timescale determine both the kinetics and the yield of a reaction. In a multilayer ice, the reaction-diffusion kinetics is dominated by the kinetics of the water ice mantle restructuration. Modeling both the statistical and kinetical aspects of reactivity is the new challenge for astrochemical models.

Acknowledgment

This work was supported by the Programme National 'Physique et Chimie du Milieu Interstellaire' (PCMI) of CNRS/INSU with INC/INP co-funded by CEA and CNES.

References

- Bacmann, A., Taquet, V., Faure, A., Kahane, C., & Ceccarelli, C. 2012, *A&A*, 541, L12
- Borget, F., Müller, S., Grote, D., P. Theulé; Vinogradoff, V., Chiavassa, T., Sander, W., *et al.* 2017, *A&A*, 598, A22
- Bossa, J. B., Theule, P., Duvernay, F., & Chiavassa, T. 2009, *ApJ*, 707, 1524
- Caselli, P. & Ceccarelli, C. 2012, *A&A Rev.*, 20, 56
- Collings, M. P., Anderson, M. A., Chen, R., Dever, J. W., Viti, S., Williams, D. A., McCoustra, M. R. S. *et al.* 2004, *MNRAS*, 354, 1133
- Cooke, I. R., Öberg, K. I., Fayolle, E. C., Peeler, Z., & Bergner, J. B. 2018, *ApJ*, 852, 75
- Ehrenfreund, P. & Charnley, S. B. 2000, *ARA&A*, 38, 427
- Goesmann, F., Rosenbauer, H., Bredehöft, J. H., *et al.* 2015, *Science*, 349, 6247
- Gudipati, M. S., Abou Mrad, N., Blum, J., *et al.* 2015, *Space Science Reviews*, 197, 101
- Ghesquière, P., Mineva, T., Talbi, D., *et al.* 2015, *PCCP*, 17, 11455
- Ghesquière P., Noble J. A., Ivlev A., & Theulé P. 2018, *A&A*, 614, A107
- He, J., Emtiaz, S. M., & Vidali, G. 2018, *ApJ*, 863, 156
- Karssemeijer, L. J., Ioppolo, S., van Hemert, M. C., van der Avoird, A., Allodi, M. A., Blake, G. A., & Cuppen, H. M. 2014, *ApJ*, 781, A16
- Livingston, F. E., Smith, J. A., & George, S. M. 2002, *J. Phys. Chem. A*, 106, 6309
- May, R. A., Smith R. S., Kay B. D. *et al.* 2013, *J. Chem. Phys.*, 138, 104501
- Mispelaer, F., Theulé, P., Aouididi, H., *et al.* 2013, *A&A*, 555, A13
- Noble, J. A., Theule, P., Duvernay, F., *et al.* 2014, *PCCP*, 16, 23604
- Oba, Y., Watanabe, N., Hama, T., Kuwahata, K., Hidaka, H., Kouchi, A., *et al.* 2012, *ApJ*, 749, 67
- Potapov A., Theulé P., Jäger C. & Henning T. 2019, *ApJL*, 878, L20
- Smith R. S., Huang C., Wong E. K. L., Kay B. D. 1997, *Phys. Rev. Lett.*, 79, 909
- Theulé, P., Duvernay, F., Danger, G., *et al.* 2013, *Advances in Space Research*, 52, 1567
- Theulé, P., Noble, J., Guesquiere, P. 2018, *Laboratory Astrophysics, Astrophysics and Space Science Library*, 451
- Viti, S., Collings, M. P., Dever, J. W., McCoustra, M. R. S., Williams, D. A., 2004, *MNRAS*, 354, 1141